ISSN 0036-0236, Russian Journal of Inorganic Chemistry, 2015, Vol. 60, No. 1, pp. 1–8. © Pleiades Publishing, Ltd., 2015.
Original Russian Text © L.S. Skogareva, V.K. Ivanov, A.E. Baranchikov, N.A. Minaeva, T.A. Tripol'skaya, 2015, published in Zhurnal Neorganicheskoi Khimii, 2015, Vol. 60, No. 1, pp. 3–10.

SYNTHESIS AND PROPERTIES OF INORGANIC COMPOUNDS

Effects Caused by Glutamic Acid and Hydrogen Peroxide on the Morphology of Hydroxyapatite, Calcium Hydrogen Phosphate, and Calcium Pyrophosphate

L. S. Skogareva[a], V. K. Ivanov[a, b], A. E. Baranchikov[a], N. A. Minaeva[a], and T. A. Tripol'skaya[a]

[a] *Kurnakov Institute of General and Inorganic Chemistry, Russian Academy of Sciences, Leninskii pr. 31, Moscow, 119991 Russia*
[b] *National Research Tomsk State University, Tomsk, Russia*
e-mail: skog@igic.ras.ru

Received June 30, 2014

Abstract—Reacting hydroxyapatite with H_2O_2 vapor at 10°C and brushite $CaHPO_4 \cdot 2H_2O$ with 90% H_2O_2 solution at 0°C (the hydroxyapatite and brushite were both prepared in the presence of glutamic acid) yielded the relevant peroxo solvates containing up to 18% hydrogen peroxide. The peroxo compounds and their degradation products obtained at 170–960°C were morphologically studied (using SEM). The factors influencing particle sizes are considered.

DOI: 10.1134/S0036023615010179

Design of biocomposites for clinical medicine relates to design of implants to imitate the natural bone tissue with its intrinsic characteristics, including the calcium phosphate composition, biocompatibility, biodegradability, the absence of immunologic or irritating effect, and nontoxicity. Synthetic hydroxyapatite is known to approach these requirements to the greatest extent. In the context of morphology, bone substitutes are to be nanostructured, as the native bone tissue. A possible route to calcium phosphate nanocrystals can appear template synthesis, as demonstrated by some researchers for hydroxyapatite and polymers, for example polyethylene, polymethacrylate, polyamide, and gelatin [1–5]. Earlier, we employed amino acids as templates to prepare calcium polyphosphates, namely glycine, L-aspartic acid, L-glutamic acid, and ε-aminocaproic acid [6]. Good results were obtained with glutamic acid ($C_5H_9NO_4$, Glu), whose structuring function is performed, as in other amino acids, due to the active sites (COOH, NH_2) where calcium phosphate particles crystallize. Glutamic acid was also chosen to serve in the template synthesis of hydroxyapatite.

Numerous studies of hydroxyapatite composites showed that the material is responsive to interaction with a bone tissue only when it comprises a biodegradable phase, which is usually tricalcium phosphate, phosphate glasses, or carbonated hydroxyapatite. Tricalcium pyrophosphate was regarded to be one such additive [7–11]. There are some grounds for this, because the complex mineralization process in a living organism involves, in particular, calcium pyrophosphate formation. An adverse factor is a possibility that pyrophosphate would pile up in the synovial fluid of joints, leading to arthritis. In order to increase the resorbability of calcium pyrophosphate, it is advisable to blend it with sodium pyrophosphate [12, 13]; such the bioceramics also have improved mechanical properties [14]. Calcium pyrophosphate glass ceramics have biological activity [15, 16]. Here, we test calcium hydrogen phosphate (brushite), which converts to pyrophosphate at high temperatures, as a potential component of biocomposites.

It would be useful to provide for the antiseptic safety of the material in design of medical implants by means of introducing a bactericide into the composite, namely hydrogen peroxide. Unlike cells where the inactivation of an oxidizing agent by means of natural or artificial antioxidants is vitally important, it is desirable that biocomposites have small concentrations of active oxygen, which has bactericidal properties. In those materials whose production requires high temperatures, the hydrogen peroxide contained therein will also perform as a pore former due to decomposition with oxygen evolution. Earlier [17] we studied formation conditions for peroxo solvates of hydroxyapatite and calcium hydrogen phosphate and some of their characteristics. The results of that study were used here.

Here, we prepared hydroxyapatite and calcium hydrogen phosphate in the presence of glutamic acid

and their peroxo derivatives to serve as precursors for microdisperse and nanodisperse materials. The above-described approach to the synthesis of bioactive materials comprises three resorbability-enhancing factors, namely: (1) decreasing particle sizes to nanometric sizes using template synthesis, (2) using hydroxyapatite with brushite mixtures, and (3) increasing porosity on account of the decomposition of solvating hydrogen peroxide at elevated temperatures.

EXPERIMENTAL

The chemicals used in the study were $CaCl_2$ (pure grade), $(NH_4)_2HPO_4$ (chemically pure grade), L-glutamic acid ($C_5H_9NO_4$, Glu) (from Sigma), and 90% and 96% hydrogen peroxide solutions. Distilled water was boiled to remove CO_2.

Hydroxyapatite synthesis was based on the protocol published in [17]. Aqueous solutions were prepared from stoichiometric amounts of $CaCl_2$ (0.2 M) and $(NH_4)_2HPO_4$ (0.04 M) (Ca : PO_4 = 1.67 : 1). Each solution was adjusted to pH of 10–12 by addition of 26% aqueous ammonia. To the calcium salt solution, was added 0.003 M glutamic acid solution (Ca : Glu = 10). Then, synthesis was carried out in two versions: (a) at room temperature and (b) while cooling the precursor solutions to 10°C. To the solution of the calcium salt with glutamic acid stirred with a magnetic stirrer and maintained at the appropriate temperature, was added an ammonium hydrogen phosphate solution, and the resulting suspension was allowed to stand (a) at room temperature for 24 h or (b) in a refrigerator (8°C) for 1 h. Further, the solid phase was filtered out was added with water until the absence of chloride ion test. The thus-obtained gel was dried to constant weight at room temperature. The composition of the material corresponded to the formula $Ca_5(PO_4)_3(OH) \cdot 0.5H_2O$; the presence of water was confirmed IR spectroscopically (the δ(H–O–H) band appeared at 1640 cm^{-1}).

Hydroxyapatite peroxo solvates were prepared by saturating solid hydroxyapatite samples with hydrogen peroxide vapor at 10°C inside a desiccator with 95% H_2O_2 solution and anhydrone.

Brushite $CaHPO_4 \cdot 2H_2O$ was prepared by reacting aqueous (0.1 M) solutions of equimolar amounts of calcium chloride and diammonium phosphate at room temperature in the presence of glutamic acid (1 mmol per 10 mmol $CaCl_2$), or without it. The solid was separated by filtration, then washed with water until the test for chloride ion was negative, and dried in air.

The reaction of $CaHPO_4 \cdot 2H_2O$ with hydrogen peroxide vapor yields a peroxo solvate with low H_2O_2 percentage (~2%). Therefore, in order to obtain peroxidated calcium hydrogen phosphate having a noticeable active oxygen content, brushite was reacted with 90% H_2O_2 solution at 0°C. After the suspension was filtered at 0°C, the residue on a glass filter was washed with cool ethanol and diethyl ether and then dried over anhydrone inside a vacuum desiccator. The composition of the thus-prepared material corresponded to the formula $CaHPO_4 \cdot 0.8H_2O_2 \cdot 1.2H_2O$ (15.1% H_2O_2).

Chemical analysis. PO_4^{3-} was determined gravimetrically through precipitation of magnesium ammonium phosphate followed by calcination thereof to $Mg_2P_2O_7$, Ca^{2+} was determined gravimetrically as calcium oxalate [18]. Active oxygen was determined permanganatometrically [19, 20].

IR spectra of solids were recorded as KBr disks on a Specord M-80 spectrophotometer in the range from 400 to 4000 cm^{-1}.

X-ray diffraction patterns of powders were recorded on a Rigaku X-ray diffractometer equipped with a RINT 2000 goniometer (CuK_α radiation, 50 kV on the anode, anodic current: 250 mA); 2θ range: 10°–90°.

Thermogravimetric curves (for ~5-g samples) were recorded on an SDT Q 600 (TA Instruments) TGA/DTA/DSC thermal analyzer in the temperature range 20–600°C at 3 K/min.

Microstructure was studied by scanning electron microscopy (SEM) using a Carl Zeiss NVision 40 workstation at an accelerating voltage of 1 kV without pre-sputtering a conductive material on the surface. Samples were partially degraded under the electronic beam while images of peroxo solvates were recorded.

RESULTS AND DISCUSSION

Hydroxyapatite (HA) was prepared by reacting calcium chloride with diammonium phosphate in an ammoniac medium in the presence of L-glutamic acid. The reaction product at 8°C was amorphous hydroxyapatite (Fig. 1, curve *1*), the product obtained at room temperature was crystalline-amorphous hydroxyapatite (Fig. 1, curve *2*). The samples were substantially free of glutamic acid (only trace amounts were observed). While developing methods for preparing peroxidated hydroxyapatites, we discovered that these compounds can be prepared by a heterophase reaction via saturating hydroxyapatite powders with H_2O_2 vapor at 10°C; this yielded peroxo solvates containing up to 18% hydrogen peroxide. Earlier [17] we used 12–99% H_2O_2 solutions for this purpose.

Since high-temperature ceramics are used to substitute for bone defects, the amorphous and amorphous-crystalline hydroxyapatite samples prepared here in the presence of glutamic acid, as their peroxidated derivatives, were heated to 960°C. Crystalline hydroxyapatite was formed in all cases (Fig. 1, curve *3*). X-ray diffraction patterns and IR spectra of crystalline hydroxyapatite samples coincided with those reported by us earlier [17] and with data published by other

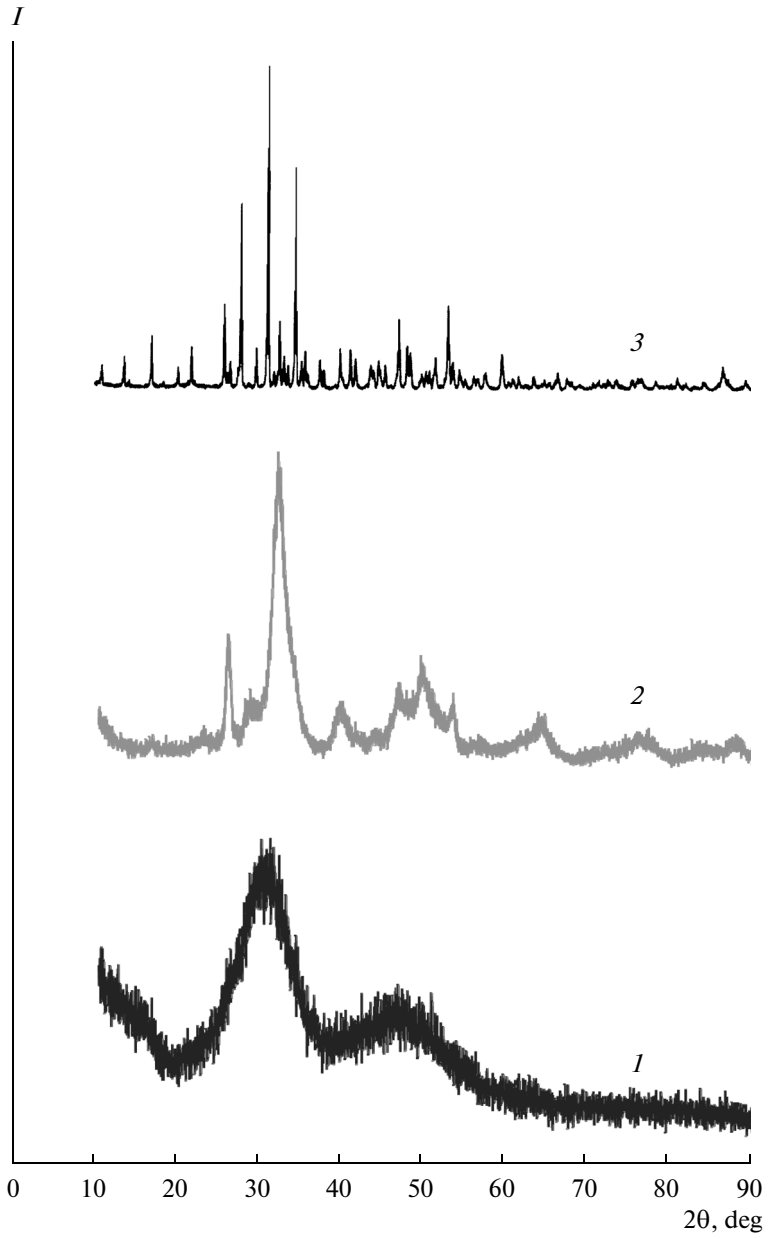

Fig. 1. X-ray diffraction patterns of (*1*) amorphous, (*2*) crystalline-amorphous, and (*3*) crystalline hydroxyapatite samples prepared by calcination at 960°C of peroxidated amorphous hydroxyapatite (5.24% H_2O_2).

researchers [21–29]. The SEM study showed that the powder obtained from an amorphous sample consisted of discrete particles with sizes of ~800 nm in length and ~150 nm in cross section (Fig. 2a). Peroxidated amorphous hydroxyapatites containing 5.24% H_2O_2, which were exposed at 960°C, typically had a more uniform powder morphology (Figs. 2b, 2c). Meanwhile, in a peroxo solvated amorphous hydroxyapatite sample (7.26% H_2O_2) that was prepared without Glu and heated at 960°C, the constituent particles were grown together to form a porous framework (Fig. 2d). These results imply that, of the two factors (H_2O_2 and glutamic acid), the template is of the greatest importance for nanostructured hydroxyapatite samples to be obtained.

In a crystalline-amorphous hydroxyapatite sample prepared in the presence of Glu which contained 2.67% H_2O_2 and was heated to 960°C, particles were joined into a loose structured network with pore sizes of 70–150 nm (Fig. 3a). In the absence of hydrogen peroxide in the precursor material, hydroxyapatite particles had far lower porosities (Fig. 3b).

Summing up the results obtained by SEM, we may speak of the following. Firstly, glutamic acid is a struc-

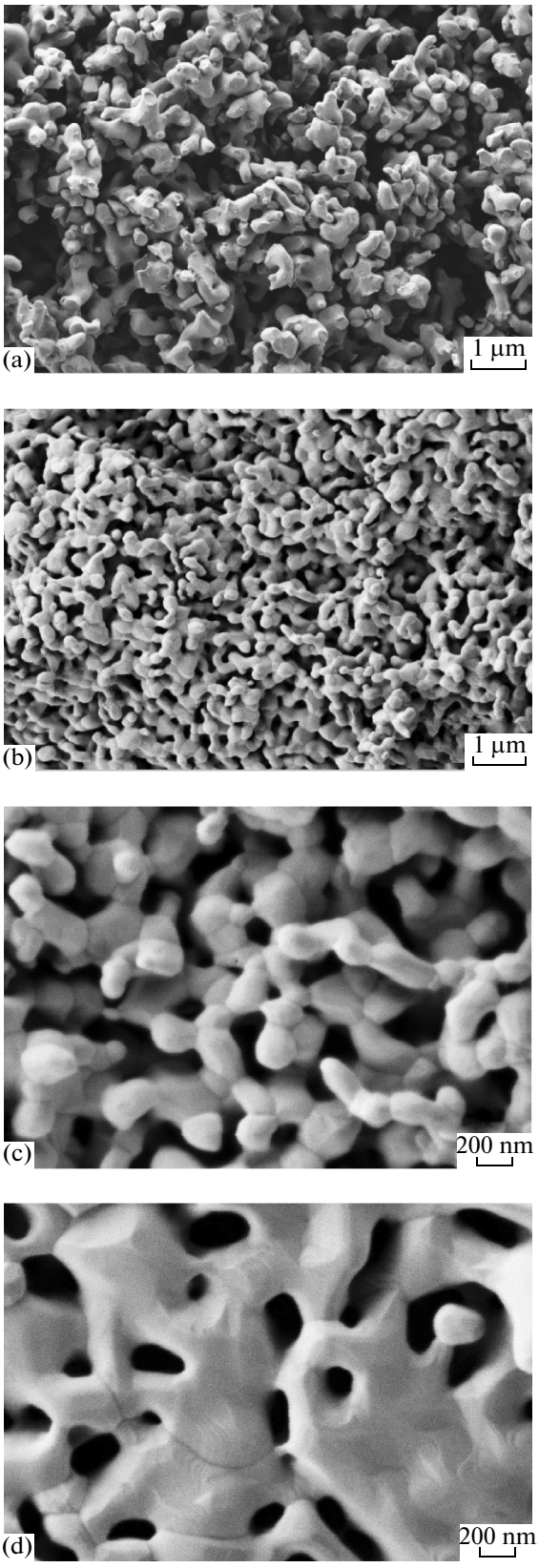

Fig. 2. SEM images of samples after exposure to 960°C: (a) amorphous hydroxyapatite prepared on a Glu template, (b, c) its peroxo derivative (5.24% H_2O_2), and (d) a peroxo derivative (7.26% H_2O_2) of amorphous HA prepared without glutamic acid.

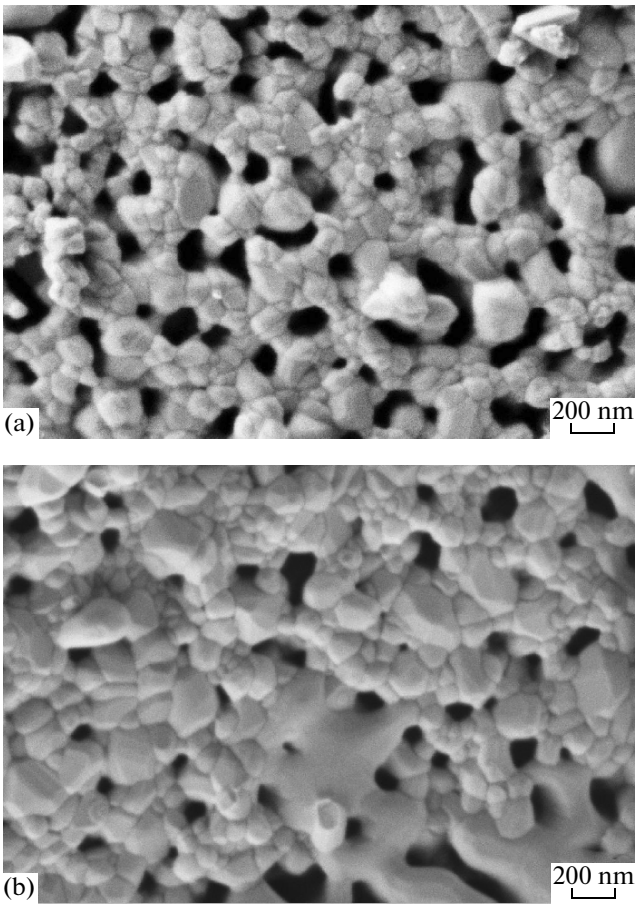

Fig. 3. SEM images of crystalline-amorphous hydroxyapatite samples prepared in the presence of glutamic acid (a) comprising 2.67% H_2O_2 and (b) without H_2O_2, recorded after heating the samples at 960°C.

turing agent in the synthesis of crystalline hydroxyapatite, and secondly, there are greater opportunities to influence the morphology in case of amorphous hydroxyapatite compared to amorphous-crystalline species. Network structures are typical of samples in the absence of one of the two factors, either glutamic acid, or hydrogen peroxide. The effect of hydrogen peroxide is likely manifested as pore formation due to H_2O_2 decomposition with evolution of oxygen and water vapor.

Calcium hydrogen phosphate (brushite) is known to lose water when heated to 100°C [7, 30, 31]. Anhydrous calcium hydrogen phosphate (monetite) transforms to γ-$Ca_2P_2O_7$ (orthorhombic) in the temperature range 270–500°C, to β-$Ca_2P_2O_7$ (tetragonal) at 500–750°C, and to α-$Ca_2P_2O_7$ (monoclinic) at 1165–1170°C. For the same transformations in monetite, temperature ranges were reported to be <627, 627–1140, and 1140–1353°C, respectively [12].

In order to prepare calcium pyrophosphate, we thermolyzed a peroxidated brushite sample of compo-

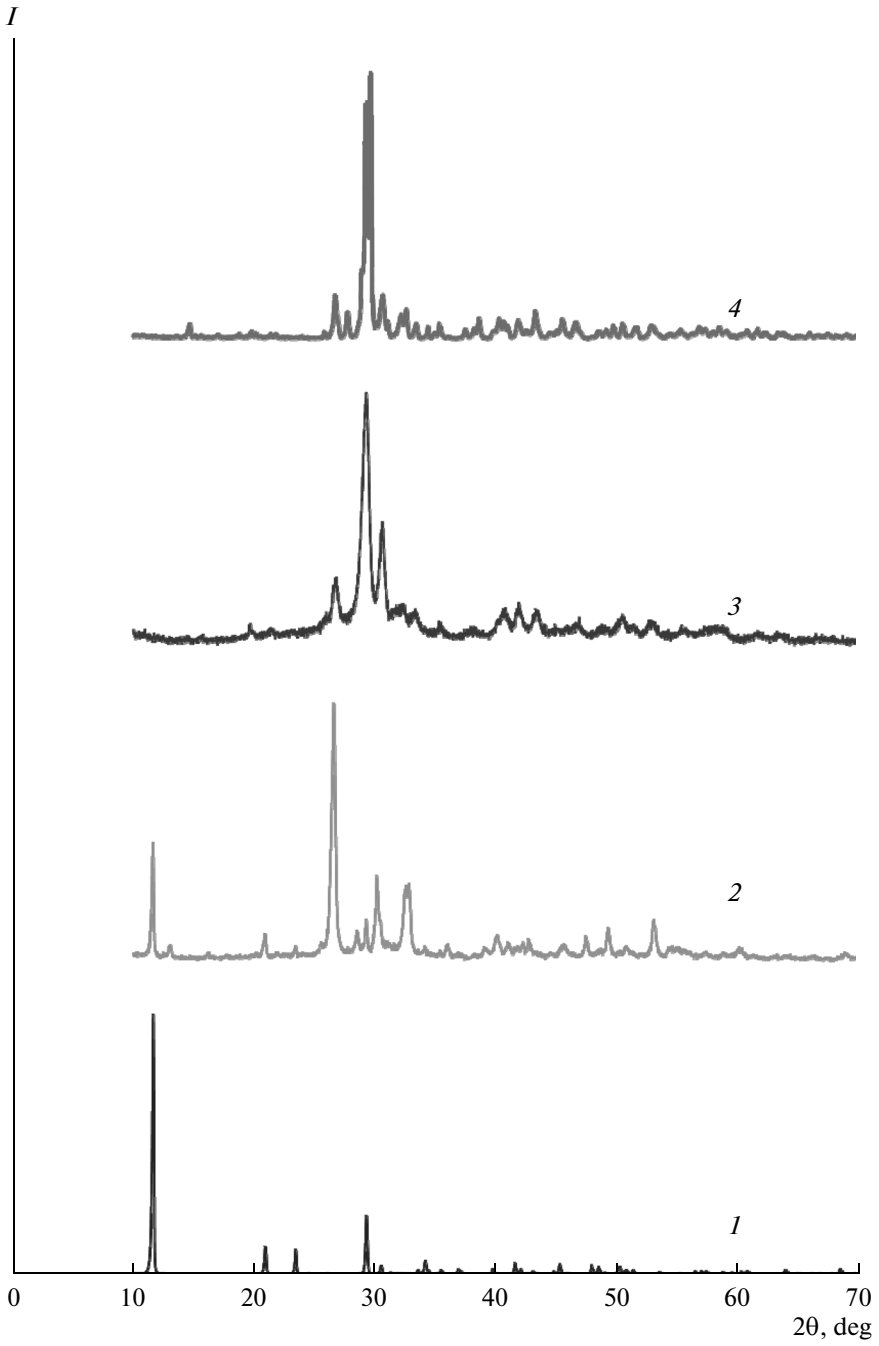

Fig. 4. X-ray diffraction patterns of (*1*) a $CaHPO_4 \cdot 2H_2O$ (brushite) sample and (*2, 3, 4*) a calcium hydrogen phosphate peroxo solvate (15.1% H_2O_2) sample recorded after heating the samples at (*2*) 170°C, (*3*) 440 (γ-$Ca_2P_2O_7$), and (*4*) 800°C (β-$Ca_2P_2O_7$). See: (*1*) PDF 01-072-0713, (*2*) PDF 01-070-0359, (*3*) PDF 00-015-0197, and (*4*) PDF 00-009-0346.

sition $CaHPO_4 \cdot 0.8H_2O_2 \cdot 1.2H_2O$. According to our data [17], the DTA curve for the peroxo solvate features one exotherm at 135–145°C (the decomposition of the peroxide component on the background of dehydration) and two endotherms at 145–150°C (the end of dehydration) and at 400–420°C (degradation to calcium pyrophosphate). Here, we heated a $CaHPO_4 \cdot 0.8H_2O_2 \cdot 1.2H_2O$ (15.1% H_2O_2) sample at 170°C; hydrogen peroxide decomposed, and the degradation product (monetite) contained minor brushite (Fig. 4; curves *1*, *2*). Exposure of $CaHPO_4 \cdot 0.8H_2O_2 \cdot 1.2H_2O$ at 440°C (in choosing this temperature, we were guided, apart from our study, by the range 325–450°C reported in [32]), brings about the formation of γ-$Ca_2P_2O_7$ (Fig. 4, curve *3*). Scanning electron microscopy showed that the resulting γ-$Ca_2P_2O_7$ had

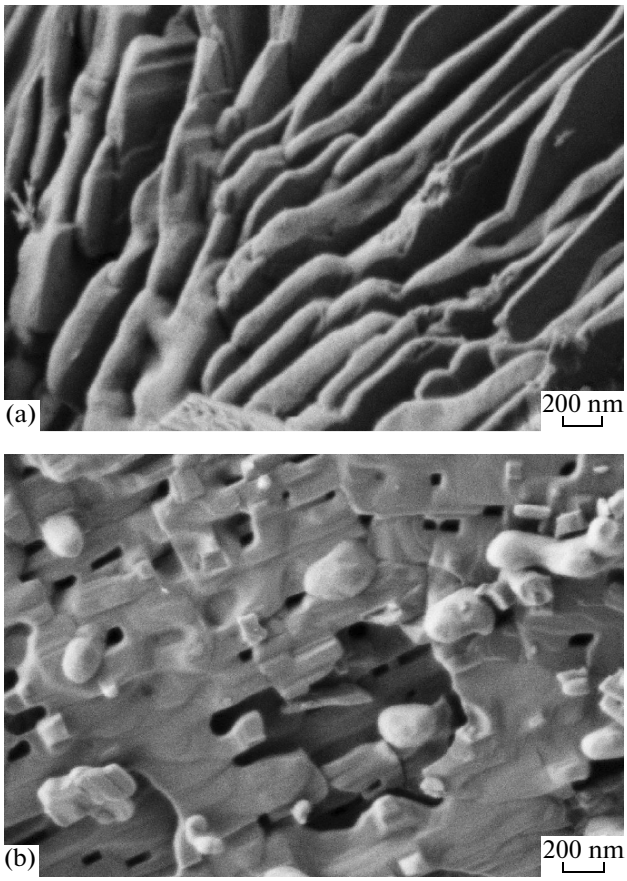

Fig. 5. SEM images of $CaHPO_4 \cdot 0.8H_2O_2 \cdot 1.2H_2O$ (15.1% H_2O_2) samples (prepared without Glu) that were exposed to (a) 440°C and (b) 800°C.

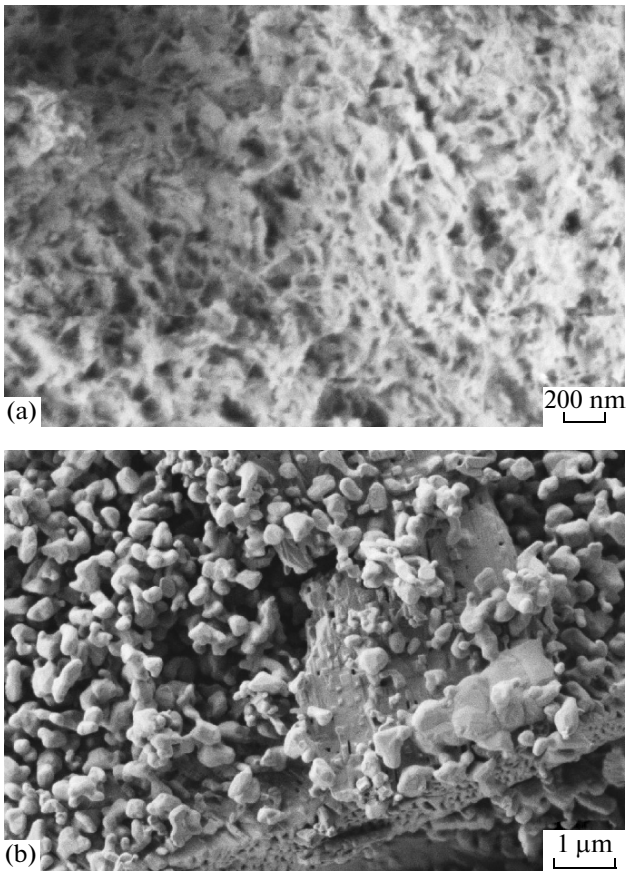

Fig. 6. SEM images of (a) a brushite sample obtained on a Glu template and (b) its degradation product at 800°C.

platy structure with platelet thicknesses of 50–150 nm (Fig. 5a). At 800°C platelets were baked to form nanopores (Fig. 5b); the X-ray powder pattern corresponded to β-$Ca_2P_2O_7$ (Fig. 4, curve *4*).

Vibration frequencies (cm^{-1}) in the IR spectrum of $Ca_2P_2O_7$

	Assignment		Assignment
452 s		1000 s	
496 vs		1032 s	
536	$\delta(PO_3)$ and $\rho(O-PO_3)$	1076 vs	
564 vs		1136	$\nu(PO_3)$
592		1168 vs	
610		1186	
724 vs		1208 s	
952 vs	$\nu(P-O-P)$		
972			

The next set of experiments was carried out using glutamic acid. The brushite sample prepared in the presence of glutamic acid was nanostructured as probed by SEM (unlike the brushite prepared in the absence of Glu, which had crystal sizes of 4–10 μm); the β phase of calcium pyrophosphate obtained from that brushite at 800°C consisted of isotropic particles with sizes of up to 0.5 μm (Fig. 6). In the IR spectrum of β-$Ca_2P_2O_7$ (Fig. 7), the characteristic vibration $\nu(PO_3)$ in $P_2O_7^{4-}$ (at 1185 cm^{-1} [31, 33]) appeared as a strong, split band at 1136–1186 cm^{-1} (table); the HPO_4^{2-} band at 866 [11] or 875 [33] cm^{-1} did not appear.

When all of the three factors are operating together (glutamic acid in the synthesis of brushite, hydrogen peroxide in the preparation of a peroxo derivative from brushite, and temperature), nanoparticles were not observed to form: at 440°C orthorhombic $Ca_2P_2O_7$ was formed as a porous mass, and at 800°C the product was tetragonal $Ca_2P_2O_7$, which had micromorphology coincident the pyrophosphate prepared without H_2O_2 (Fig. 6b).

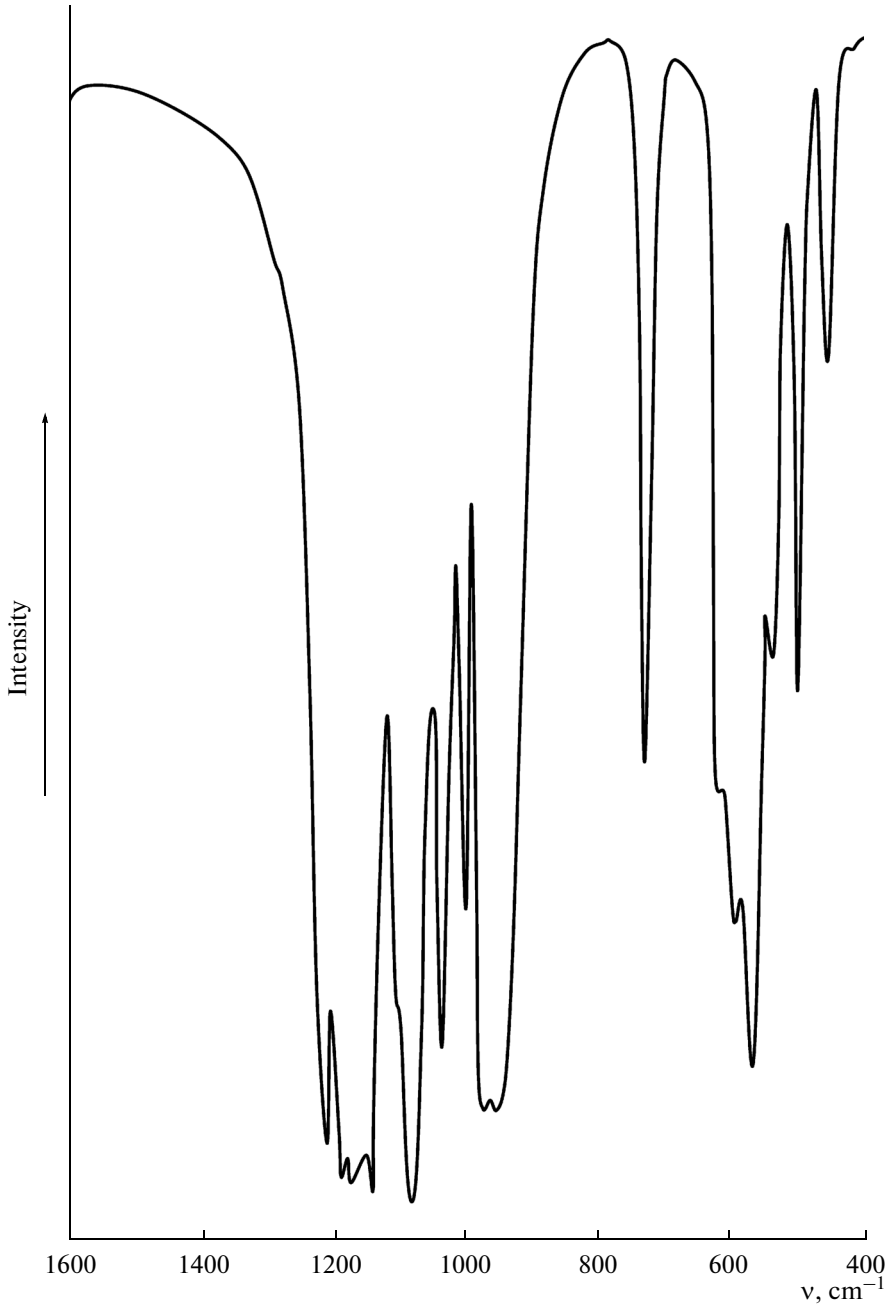

Fig. 7. IR spectrum of $Ca_2P_2O_7$.

In summary, we have prepared micro- and nanosized hydroxyapatite and calcium pyrophosphate in the presence of glutamic acid. Peroxo derivatives make it possible to increase the porosity of the material. A variable combination of three factors (Glu, H_2O_2, and temperature) offers a means to influence the morphologies of the compounds studied. Peroxidated hydroxyapatites having noticeable hydrogen peroxide percentages are also formed in reaction both with 12–99% H_2O_2 solutions and with saturated H_2O_2 vapor. In case of brushite, the reaction occurs only in solution. It seems promising to investigate the effects of other amino acids and of polysaccharides on the crystallization of the compounds studied.

ACKNOWLEDGMENTS

This study was performed under the auspice of the Fundamental Research Program of the Presidium of the Russian Academy of Sciences “Development of Methods for Preparing Chemical Compounds and Materials Design.”

REFERENCES

1. G. V. Rodicheva, V. P. Orlovskii, V. I. Privalov, et al., Russ. J. Inorg. Chem. **46**, 1631 (2001).
2. S. M. Barinov, Ross. Khim. Zh. (Zh. Ross. Khim. O–va im. D.I. Mendeleeva) **53** (2), 123 (2009).
3. S. M. Barinov, Usp. Khim. **79**, 15 (2010).
4. N. Roveri, G. Falini, M. C. Sidoti, et al., Mater. Sci. Eng., 441 (2003).
5. M. Kikuchi, S. Itoh, S. Ichinose, et al., Biomaterials **22**, 1705 (2001).
6. L. S. Skogareva, V. K. Ivanov, O. S. Ivanova, et al., Neorg. Mater. **49**, 871 (2013).
7. T. V. Safronova, V. I. Putlyaev, M. A. Shekhirev, et al., Steklo Keram., No. 3, 31 (2007).
8. E. S. Kovaleva, M. P. Shabanov, V. I. Putlyaev, et al., Materialwis. Werkstoff. **39**, 822 (2008).
9. E. S. Kovaleva, M. P. Shabanov, V. I. Putlyaev, et al., Centr. Eur. J. Chem. **7**, 168 (2009).
10. T. V. Safronova and V. I. Putlyaev, Nanosistemy: Fiz., Khim., Mat. **4**, 24 (2013).
11. H. Zhao, W. He, Y. Wang, et al., Mat. Chem. Phys. **111**, 265 (2008).
12. V. Vincent, G. Nihoul, and J. R. Gavarri, Solid State Ion. **92**, 11 (1996).
13. F. -H. Lin, C.-J. Liao, K. S. Chen, et al., Biomaterials **18**, 915 (1997).
14. F. H. Lin, J. R. Liaw, M. H. Hon, et al., Mater. Chem. Phys. **41**, 110 (1995).
15. T. Kasuga, M. Nogami, and M. Niinomi, J. Mater. Sci. Lett. **20**, 1249 (2001).
16. T. Kasuga, Acta Biomater. **1**, 55 (2005).
17. L. S. Skogareva, G. P. Pilipenko, I. V. Shabalova, et al., Russ. J. Inorg. Chem. **56**, 673 (2011).
18. G. Charlot, *Les Methodes de la Chimie Analytique: Analyse Quantitative Minerale* (Masson, Paris, 1961), Vol. 2.
19. W. C. Schumb, Ch. N. Satterfield, and R. L. Wentworth, *Hydrogen Peroxide* (Reinhold, New York, 1955; Inostrannaya Literatura, Moscow, 1958).
20. *Hydrogen Peroxide and Peroxide Compounds*, Ed. by M. E. Pozin (Goskhimizdat, Moscow, 1951) [in Russian].
21. C. Jager, T. Welzel, W. Meyer-Zaika, et al., Magn. Reson. Chem. **44**, 573 (2006).
22. H. Yu, H. Zhang, X. Wang, et al., J. Phys. Chem. Solids **68**, 1863 (2007).
23. D. Tadic, F. Peters, and M. Epple, Biomaterials **23**, 2553 (2002).
24. H. Zhao, X. Li, J. Wang, et al., J. Biomed. Mater. Res. **52**, 157 (2000).
25. K. C. Blakeslee and R. A. Condrate, J. Am. Ceram. Soc. **54**, 559 (1971).
26. B. O. Fowler, Inorg. Chem. **13**, 194 (1974).
27. N. A. Chumaevskii, V. P. Orlovskii, Zh. A. Ezhova, et al., Zh. Neorg. Khim. **37**, 1455 (1992).
28. P. F. Gonzalez-Diaz and M. Santos, J. Solid State Chem. **22**, 193 (1977).
29. G. Engel and W. E. Klee, J. Solid State Chem. **5**, 28 (1972).
30. T. Kanazava, *Inorganic Phosphate Materials* (Naukova Dumka, Kiev, 1998) [in Russian].
31. J.-J Bian, D.-W. Kim, and K.S. Hong, J. Eur. Ceram. Soc. **23**, 2589 (2003).
32. B. O. Fowler, E. C. Moreno, and W. E. Brown, Arch. Oral. Biol. **11**, 477 (1996).
33. F.-H. Lin, C.-J. Liao, and K.-S. Chen, Biomaterials **19**, 1101 (1998).

Translated by O. Fedorova